Available online at www.sciencedirect.com
SCIENCE DIRECT
Biochemical and Biophysical Research Communications 339 (2006) 79–88
BBRC
www.elsevier.com/locate/ybbrc

Hepatocyte-specific deletion of the *keap1* gene activates Nrf2 and confers potent resistance against acute drug toxicity

Hiromi Okawa [a], Hozumi Motohashi [a,*], Akira Kobayashi [a], Hiroyuki Aburatani [b], Thomas W. Kensler [c], Masayuki Yamamoto [a,d,*]

[a] *Graduate School of Comprehensive Human Sciences, Center for Tsukuba Advanced Research Alliance, University of Tsukuba, 1-1-1 Tennoudai, Tsukuba 305-8577, Japan*
[b] *Research Center for Advance Science and Technology, The University of Tokyo, Tokyo 153-8904, Japan*
[c] *Department of Environmental Health Sciences, Bloomberg School of Public Health, Johns Hopkins University, Baltimore, MD 21205, USA*
[d] *ERATO Environmental Response Project, Japan Science and Technology Corporation, 1-1-1 Tennoudai, Tsukuba 305-8577, Japan*

Received 25 October 2005
Available online 8 November 2005

Abstract

Nrf2 is a key regulator of many detoxifying enzyme genes, and cytoplasmic protein Keap1 represses the Nrf2 activity under quiescent conditions. Germ line deletion of the *keap1* gene results in constitutive activation of Nrf2, but the pups unexpectedly died before weaning. To investigate how constitutive activation of Nrf2 influences the detoxification system in adult mice, we generated mice bearing a hepatocyte-specific disruption of the *keap1* gene. Homozygous mice were viable and their livers displayed no apparent abnormalities, but nuclear accumulation of Nrf2 is elevated. Microarray analysis revealed that, while many detoxifying enzyme genes are highly expressed, some of the typical Nrf2-dependent genes are only marginally increased in the Keap1-deficient liver. The mutant mice were significantly more resistant to toxic doses of acetaminophen than control animals. These results demonstrate that chronic activation of Nrf2 confers animals with resistance to xenobiotics without affecting the morphological and physiological integrity of hepatocytes.

Keywords: Nrf2; Keap1; Alb-Cre; Conditional knockout mice; Acetaminophen; Hepatotoxicity; ARE; Phase2 enzymes; GST; UGT

Drug-metabolizing enzymes are central to the detoxification and elimination of xenobiotics introduced into our body as food, medicine or environmental pollutants [1]. The susceptibility of animals to drug toxicity is often dependent on the activities of their drug-metabolizing enzymes [2,3]. The detoxification process conceptually comprises three sequential reactions, referred to as Phase 1, 2, and 3 metabolism. In the Phase 1 reaction, xenobiotics are metabolized by the cytochrome P450 (CYP) system to add or expose functional groups. The products are, in some cases, highly reactive and can easily bind to cellular proteins or DNA, resulting in cytotoxicity and carcinogenesis. These products of Phase 1 metabolism have the ability to induce enzymes of the Phase 2 system due to their electrophilic nature. The Phase 2 enzymes, including glutathione *S*-transferase (GST), UDP-glucuronosyltransferase (UGT), sulfotransferase (SULT), and NADP(H):quinone oxidoreductase 1 (NQO1), catalyze the conversion or conjugation of the reactive Phase 1 metabolites to more hydrophilic and stable products [4]. In the Phase 3 reaction, xenobiotic conjugates and metabolites are expelled by membrane efflux pumps that include the multi-drug resistance-associated proteins [5]. Phase 2 and Phase 3 reactions are considered to be important in avoiding tissue injury through their respective activities of conjugation and elimination.

The Nrf2 transcription factor belongs to the cap-n-collar family of activators, characterized by a highly conserved basic region-leucine zipper structure [6]. The transcriptional activity of Nrf2 requires prior dimerization with a member of the small Maf protein family to allow interaction with the

* Corresponding authors. Fax: +81 29 853 7318.
E-mail address: masi@tara.tsukuba.ac.jp (M. Yamamoto).

0006-291X/$ - see front matter © 2005 Elsevier Inc. All rights reserved.
doi:10.1016/j.bbrc.2005.10.185

antioxidant or electrophile responsive element (ARE/EpRE) [7,8]. Nrf2 coordinately regulates the gene expression of a battery of Phase 2 enzymes through ARE sequences within their gene-regulatory regions [9]. In addition, a recent study suggests that Nrf2 regulates expression of one of the Phase 3 transporters [10]. The importance of these ARE-dependent gene products has been clearly demonstrated through analyses of *nrf2*-null mutant mice, which are highly susceptible to acute toxicity caused by acetaminophen [11,12], diesel exhaust [13] or 2,3-butyl-4-hydroxytoluene [14]. Through its ability to mediate the induction of a battery of Phase 2 enzymes, Nrf2 is an indispensable regulator for the defense mechanism against xenobiotics.

The cytoplasmic protein Keap1 directly binds to Nrf2 and represses transactivation by promoting proteasome-dependent degradation of the protein [15–17]. Several lines of recent evidence revealed that Keap1 is an adaptor molecule for the Cullin3-based E3 ubiquitin ligase complex and directs the rapid degradation of Nrf2 [18]. When cells are exposed to electrophiles, Nrf2 is liberated from the Keap1-mediated degradation process and accumulates in the nucleus to activate ARE-mediated gene transcription.

We previously generated *keap1* gene knockout mice, expecting that high-level expression of Nrf2–ARE target genes might be achieved in the absence of Keap1 and that *keap1*-null mutant mice would be very resistant to xenobiotic toxicity. However, we found that Keap1-deficient mice died before weaning due to the hyperkeratotic lesions in the esophagus and forestomach, which led to obstruction of the upper digestive tract [19]. Nonetheless, we could observe a constitutive increase of ARE-dependent gene expression in *keap1*-null mutant pups and embryonic fibroblasts [19]. The phenotypes observed in the *keap1*-null mice, such as lethality before weaning, hyperkeratotic lesions, and the constitutive increase of the ARE-dependent gene expression, were all alleviated by the simultaneous disruption of the *nrf2* gene [19], demonstrating that Nrf2 is essentially the only target molecule of Keap1. Thus, the *keap1*-null background provides an environment where Nrf2 may be stabilized and thereby localize to the nucleus, where it activates transcription without requiring any exogenous stimuli. Unfortunately, premature death precluded the utilization of this line of mice harboring the simple *keap1* gene disruption from further studies, especially those concerned with the consequence of constitutive Nrf2 activation.

Acetaminophen (APAP) is a widely used nonprescription drug with analgesic and antipyretic properties. When used at therapeutic doses, the principal route of excretion is glucuronidation (52–57% total urinary metabolites) with a lesser contribution by sulfation (30–44%) and oxidation (<5%) [20,21]. When used at higher doses, an increased amount of APAP is oxidized to the highly reactive metabolite, *N*-acetyl-*p*-benzoquinone imine (NAPQI) [20,22]. NAPQI is normally detoxified through conjugation with glutathione (GSH) [23]. However, in situations where NAPQI formation exceeds the hepatic capacity of cellular GSH or when cellular GSH production and conjugation systems are defective, NAPQI covalently binds to cellular proteins and forms adducts, which provoke cytotoxicity. It has long been known that pharmacological inducers of Phase 2 enzymes protect against APAP hepatotoxicity in mice [24,25]. Conversely, we and one other group have shown that Nrf2-null mutant mice are more sensitive to APAP hepatotoxicity [11,12].

To examine in detail how constitutive activation of Nrf2 influences cellular defense mechanisms, especially in the hepatocyte, we decided to pursue a conditional disruption strategy for the *keap1* gene and in this way avoid the lethality before weaning age. The results demonstrate that somatic inactivation of the *keap1* gene in hepatocytes does not interfere with the development or the morphological and physiological integrity of the liver, but rather leads to an activation of Nrf2–ARE pathway and acquisition of resistance against APAP toxicity.

Materials and methods

Generation of mice with floxed keap1-targeted allele and hepatocyte-specific disruption of the keap1 gene. Mouse *keap1* genomic DNA was isolated from mouse 129SvJ genomic library (Stratagene). To construct a targeting vector, we included cDNAs encoding Diphtheria toxin A (DTA) and neomycin resistance (Neo) for negative and positive selection, respectively. We constructed a triple-loxP *keap1*-targeting vector to generate a floxed mouse *keap1*-targeted locus consisting of a loxP site inserted into the third *keap1* intron and a floxed Neo cassette downstream of the terminal exon. Splicing accepter-fused EGFP cDNA was also incorporated into 3′ of the Neo cassette. DTA cassette was placed outside of the *keap1* gene homology region for negative selection. Targeting in E14 ES cells has been described [19]. After PCR screening of 310 ES clones, we identified 11 clones that carried the homologously recombined allele. ES cells with the appropriate flox *keap1*-targeted locus were identified by Southern blot analysis of *Bam*HI-digested DNA using a 5′ probe located outside the targeting vector. Three clones showed positive 16.4 and 10.5 kb fragments. Sequencing analysis confirmed that three clones included triple-loxP sites but others did not. The chimeric mice were crossed with C57/B6 wild-type mice to produce $keap1^{flox/+}$ mice. Hepatocyte-specific deletion of the *keap1* allele was accomplished through breeding with the albumin-Cre recombinase (Alb-Cre) C57/B6 transgenic mice (purchased from the Jackson Laboratory). Alb-Cre mice were crossed with $keap1^{+/-}$ mice [19] to obtain *Alb-Cre::*$keap1^{+/-}$ mice, which were then crossed with $keap1^{flox/+}$ mice to generate hepatocyte-specific *keap1*-deficient (*Alb-Cre::*$keap1^{flox/-}$) mice.

APAP treatment. Five- to six-week-old mice were treated with APAP, which was purchased from Sigma (St. Louis, MO). For the dose–response study, APAP was dissolved in saline and intraperitoneally administered to mice. At least three mice of each genotype were used at each dose. The animals were sacrificed 48 h after dosing. In the time-course study, a dose of 500 mg/kg APAP was administered to the mice and animals were sacrificed at 0 (without dosing), 2, and 5 h after dosing.

Histology and immunohistochemistry. Animals were sacrificed at the indicated times after treatment with APAP or saline. Livers were fixed in 3.7% neutral buffered formalin and imbedded in paraffin for hematoxylin/eosin staining and immunohistochemical staining. The antibody against APAP (Biogenesis, Kingston, NH) was used at 1:250 dilution, while the negative control sections were incubated in PBS. Immunoreactivity was visualized with an avidin–biotin–peroxidase kit (Vector Laboratories).

RT-PCR and RNA blot analysis. Total RNA was extracted from liver using Isogen (Nippon Gene, Toyama), and cDNA was synthesized using oligo(dT) primer. PCR primers specific to each cDNA were as follows: Keap1, 5′-ggaatgagtggcggatgatcac-3′ and 5′-gcttcagcaggtacagttttg-3′; SULT3A1, 5′-tgccatcacctcgcatcttca-3′ and 5′-ccaacaacacctttgcgaaggaaa-3′; carbonyl reductase 3 (Cbr3), 5′-caacgcgggcatcgccttta-3′ and 5′-ccctcgcc atgtcggtctt-3′; glutathione peroxidase 2 (Gpx2), 5′-gcctggatggggagaagat

ag-3′ and 5′-catgagggagaacgggtcatc-3′; GST mu3, 5′-tgattaggcccctgcc atgct-3′ and 5′-ttgggtctgggcaccaatgaa-3′; GSTmu4, 5′-cgggggttctgggaac agttg-3′ and 5′-gctggcaggcaagaccatcaa-3′; GSTmu6, 5′-tcggagttcctggg gaagc ag-3′ and 5′-cctcaaagcgggccatgaagt-3′; UGT1A10, 5′-attgccttaggc tgcac ttctg-3′ and 5′-ccac ttctc aatgggt cttgga-3′; hypoxanthine phosphoribosyltransferase (HPRT), 5′- cacaggactagaacacctgc-3′ and 5′-g ctgg tgaaaaggacctct-3′. For RNA blot analysis, total RNA (15 μg per lane) was used for electrophoresis, followed by hybridization to radio-labeled probes as described previously [9]. DNA probes for NQO1, Nrf2, catalytic subunit of glutamate-cysteine ligase (GCLC), peroxiredoxin1 (Prdx1), UGT1A total, UGT1A6, and heme oxygenase-1 (HO-1) were as described previously [11,19,26,27].

Immunoblotting analysis. The preparation of nuclear extracts from liver and immunoblotting analysis were as described previously [19,28]. Antiserum to Nrf2 was made by immunizing rabbits with the Neh2 domain of the Nrf2 protein whereas the antibody against nuclear LaminB was purchased from Santa Cruz (M-20).

Microarray analysis. Total RNA samples were extracted from four 6-week-old *Alb-Cre::keap1*$^{+/+}$ mice and two 6-week-old *Alb-Cre::keap1*$^{flox/-}$ mice. The isolated RNAs were then purified using the RNeasy Mini kit (Qiagen). Purified RNA was processed and hybridized to a mouse expression array Affymetrix Mouse Genome 430 2.0 Arrays (Affymetrix, Santa Clara, CA) that contain 45,101 probe sets. Experimental procedures for Gene Chip were performed according to the Affymetrix Technical Manual.

Biochemical analysis. Plasma alanine aminotransferase (ALT) activities were assayed as a marker of APAP-induced hepatocyte injury at 48 h after APAP treatment or saline. ALT activity was measured with an automated biochemical analyzer, DRI-CHEM 7000V (Fujifilm, Japan).

Results

Generation of hepatocyte-specific keap1-null mutant mice

To examine how constitutive activation of Nrf2 modulates the defense mechanisms against xenobiotic toxicity, we generated hepatocyte-specific *keap1*-null mutant mice using the Cre-loxP system (Fig. 1). A targeting vector was constructed in which exons 4–6 of the *keap1* locus were flanked with loxP sequences (Fig. 1A). This region encodes the double glycine repeat (DGR) domain, a region that is important for Keap1 interaction with Nrf2 [29,30]. It was expected therefore that Cre-loxP recombination would generate a truncated form of Keap1 no longer capable of repressing Nrf2 activity.

Homologous recombination between the targeting vector and the *keap1* locus in mouse ES cells was confirmed by Southern blot analysis (Fig. 1B). *Bam*HI-digested genomic DNA was hybridized to a probe complementary to the 5′ region of the *keap1* gene. Three independent homologous recombinant clones were identified by the presence of an additional shorter DNA fragment, created by the presence of a *Bam*HI site in the flanking region of the loxP element. Chimeric mice were obtained by microinjecting *keap1*$^{flox/+}$ ES cells into mouse blastocysts and the resulting animals were crossed with wild-type C57BL/6J mice to achieve germ line transmission of floxed *keap1* allele.

In preliminary experiments, *keap1*$^{flox/+}$ mice were crossed with *AYU1-Cre::keap1*$^{+/-}$ mice, which express Cre recombinase ubiquitously [31 and data not shown]. Consistent with the previous *keap1* gene knockout analysis

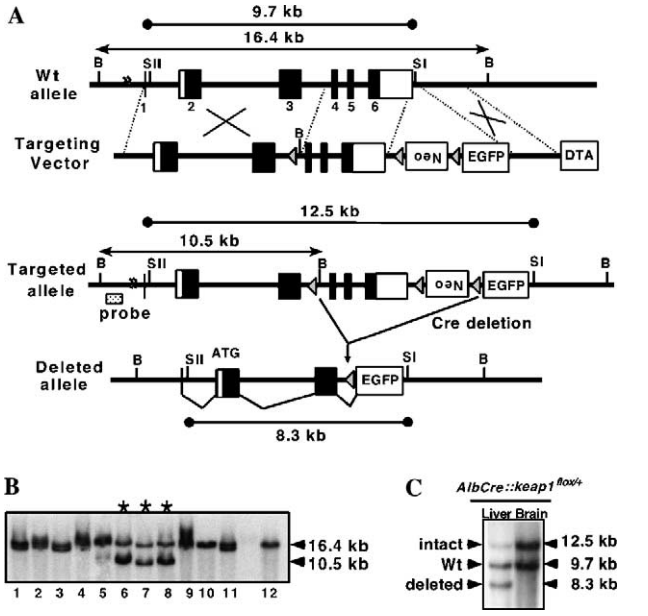

Fig. 1. Generation of *keap1* floxed mice. (A) The targeting strategy is illustrated. Structures of the *keap1* allele, *keap1*-targeting construct, floxed *keap1* allele, and floxed *keap1* allele after Cre-mediated recombination are shown. Coding exons of the mouse *keap1* gene are shown with filled boxes and the loxP sites are indicated with gray arrowheads. B, SII, and SI strand for the restriction sites of *Bam*HI, *Sac*II, and *Spe*I, respectively. A dotted bar indicates a probe used for selecting ES clones with appropriate homologous recombination. (B) Southern blot analysis showing the generation of ES clones with floxed *keap1* allele. Eleven candidate ES clones were analyzed (lanes 1–11). *Bam*HI fragments (shown as a double headed arrow in A) specific to wild-type allele (16.4 kb) and targeted allele (10.5 kb) are shown. Asterisks indicate targeted clones. Wild-type genomic DNA was used as a control (lane 12). (C) Southern blot analysis showing hepatocyte-specific recombination of the floxed *keap1* allele. DNA was purified from liver and brain of *Alb-Cre::keap1*$^{flox/+}$ mice. *Sac*II–*Spe*I fragments (shown as a horizontal bar flanked with filled circles in A) of wild-type allele (9.7 kb), targeted allele (12.5 kb), and deleted allele (8.3 kb) are shown. Note that the deleted form is only apparent in the liver DNA preparation.

[19], *AYU1-Cre::keap1*$^{flox/-}$ mice displayed severe growth retardation and lethality at the time of weaning accompanied by hyperkeratosis of the upper digestive tracts.

To generate an hepatocyte-specific line of *keap1* gene knockout mice, we crossed *keap1*$^{flox/+}$ mice with *Alb-Cre::keap1*$^{+/-}$ mice, yielding *Alb-Cre::keap1*$^{flox/+}$ mice. Southern blot analysis of *Alb-Cre::keap1*$^{flox/+}$ mice showed that hepatocyte-specific deletion of the *keap1* gene was almost completely achieved, with an estimated efficiency of more than 80% as calculated from the band intensities of intact versus deleted floxed alleles (Fig. 1C). Cell lineages, apart from hepatocytes, contained in the liver preparation, such as macrophages and endothelial cells, may account for the remaining 20% of intact floxed allele.

Expression levels of Nrf2 target genes are constitutively increased in Alb-Cre::keap1$^{flox/-}$ *mouse liver*

From mating of *keap1*$^{flox/+}$ mice with *Alb-Cre::keap1*$^{+/-}$ mice, we also obtained *Alb-Cre::keap1*$^{flox/-}$ mice, which

lack *keap1* gene expression specifically in the liver. *Alb-Cre::keap1*$^{flox/-}$ mice were viable, had normal growth rates, and appeared healthy (Fig. 2A). Their livers exhibited histological characteristics similar to those of wild-type littermates (Figs. 2B and C). Serum biochemical data were within the normal range (data not shown). RT-PCR analysis confirmed that the Keap1 mRNA level was markedly decreased in *Alb-Cre::keap1*$^{flox/-}$ mouse livers (Fig. 2D). These results thus indicate that the hepatocyte-specific depletion of Keap1 did not cause any adverse effects and further supports our conclusion that the lethality of the *keap1*-null mutant mice originated from hyperkeratosis of the upper digestive tracts.

Consistent with the notion that Keap1 sequesters and degrades Nrf2 in the cytoplasm [15,18,19], we observed markedly more abundant nuclear accumulation of Nrf2 in the *Alb-Cre::keap1*$^{flox/-}$ mouse livers when compared to those of the control animals (Fig. 2E). These results suggest that the expression level of the genes regulated by the Nrf2–ARE pathway is increased constitutively even under quiescent conditions. As expected, a typical ARE-dependent gene, *nqo1*, was highly expressed in *Alb-Cre::keap1*$^{flox/-}$ mouse livers compared to that of wild-type or *keap1* heterozygous mutant mice (Fig. 2F). Nrf2 mRNA expression was not changed substantially in all genotypes, as is the case for *keap1*-null mutant mice [19]. These results demonstrate that hepatocyte-specific depletion of Keap1 actually directs constitutive nuclear accumulation of Nrf2 and activation of ARE-dependent gene transcription.

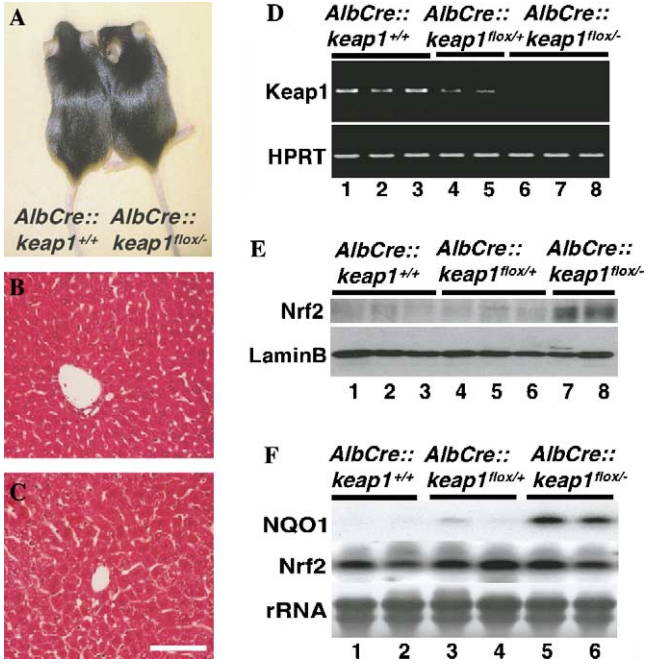

Fig. 2. Consequence of hepatocyte-specific disruption of *keap1* gene. (A) Macroscopic observation of *Alb-Cre::keap1*$^{flox/-}$ mice. (B,C) Liver sections stained with hematoxylin and eosin. Livers of wild-type (*Alb-Cre::keap1*$^{+/+}$) mouse (B) and *Alb-Cre::keap1*$^{flox/-}$ mouse (C) are shown. Scale bar corresponds to 100 μm. (D) Keap1 mRNA was detected by RT-PCR in the livers of *Alb-Cre::keap1*$^{+/+}$ (lanes 1–3), *Alb-Cre::keap1*$^{flox/+}$ (lanes 4 and 5), and *Alb-Cre::keap1*$^{flox/-}$ (lanes 6–8). HPRT expression level was examined as a loading control. (E) Immunoblotting analysis detecting nuclear accumulation of Nrf2 in the livers of *Alb-Cre::keap1*$^{+/+}$ (lanes 1–3), *Alb-Cre::keap1*$^{flox/+}$ (lanes 4–6), and *Alb-Cre::keap1*$^{flox/-}$ (lanes 7 and 8). LaminB was used as a loading control of nuclear extracts. (F) RNA blot analysis showing expressions of *nqo1* and *nrf2* genes in the livers of *Alb-Cre::keap1*$^{+/+}$ (lanes 1 and 2), *Alb-Cre::keap1*$^{flox/+}$ (lanes 3 and 4), and *Alb-Cre::keap1*$^{flox/-}$ (lanes 5 and 6) mice. The amount of ribosomal RNA was monitored as a loading control.

Microarray analysis with Keap1-deficient liver

Genetic activation of Nrf2 in hepatocytes was successfully achieved in *Alb-Cre::keap1*$^{flox/-}$ mice without the supply of any exogenous inducers. This enabled us to examine the response of the Nrf2–ARE pathway to liberation from Keap1 repression purely in the hepatocyte cell population. Therefore, we investigated comprehensively the gene expression profile of *Alb-Cre::keap1*$^{flox/-}$ mouse liver by a microarray approach (Fig. 3A). Microarray analysis was performed using RNAs from livers of *Alb-Cre::keap1*$^{flox/-}$ and *Alb-Cre::keap1*$^{+/+}$ mice. Overall, 15,493 probe sets were expressed in the *Alb-Cre::keap1*$^{+/+}$ livers (identified as "present" by Affymetrix software), whereas 16,475 probe sets were expressed in *Alb-Cre::keap1*$^{flox/-}$ livers. Expression levels of 47 genes were increased more than fourfold in the *Alb-Cre::keap1*$^{flox/-}$ livers compared with those in the *Alb-Cre::keap1*$^{+/+}$ livers, while those of 31 genes were decreased to less than one-fourth in the *Alb-Cre::keap1*$^{flox/-}$ livers.

When we categorized 47 genes in the former group according to their function (Fig. 3B and Table 1), we found 15 genes to be involved in the xenobiotic metabolism and antioxidant function, among which seven were well-

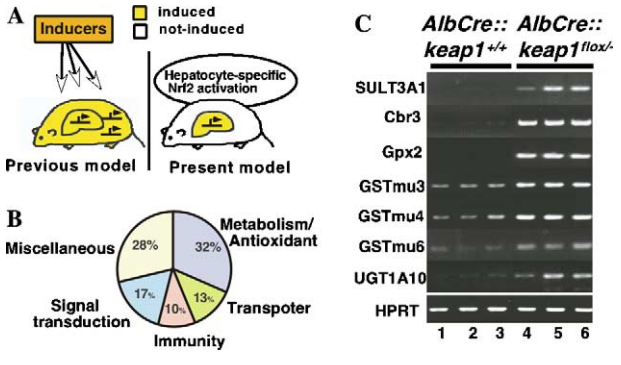

Fig. 3. Changes in the expression level of ARE-dependent genes in hepatocyte-specific *keap1*-deficient mice. Hepatic gene expression patterns were compared between 6-week-old *Alb-Cre::keap1*$^{+/+}$ and *Alb-Cre::keap1*$^{flox/-}$ mice. (A) Illustration of sample preparation for the microarray analysis. (B) Forty-eight genes increasing more than fourfold were categorized into five groups. The percentage of each category is shown. (C) The expression levels of representative genes were examined by semi-quantitative RT-PCR. cDNAs were synthesized from the liver RNAs of *Alb-Cre::keap1*$^{+/+}$ (lanes 1–3) and *Alb-Cre::keap1*$^{flox/-}$ mice (lanes 4–6). As loading controls, HPRT expression level was monitored.

Table 1
Genes expressed constitutively at higher level in *Alb-Cre::keap1*$^{flox/-}$ livers than *Alb-Cre::keap1*$^{+/+}$ livers

Description of genes	Accession No.	Fold[a]
Xenobiotic metabolism and antioxidant response		
Sulfotransferase family 2A, dehydroepiandrosterone (DHEA)-preferring, member 2	NM_009286	1782
Carbonyl reductase 3	AK003232	104
Cytochrome P450, family 2, sub-family b, polypeptide 13	NM_007813	84
Flavin containing monooxygenase 3	NM_008030	45
Cytochrome P450, family 2, sub-family b, polypeptide 9	NM_010000	18
Glutathione *S*-transferase, μ 3[b]	J03953	16
NAD(P)H dehydrogenase, quinone 1[b]	AV158882	15
Sulfotransferase family 3A, member 1	NM_020565	15
Glutathione peroxidase 2[b]	NM_030677	7.5
Microsomal glutathione *S*-transferase 3	NM_025569	6.1
Glutathione *S*-transferase, μ 4[b]	AF464943	5.3
Flavin containing monooxygenase 2	NM_018881	4.9
Glutathione *S*-transferase, μ 6[b]	NM_008184	4.6
Glutathione *S*-transferase, α 2 (Yc2)[b]	NM_008182	4.0
Glutamate-cysteine ligase, catalytic subunit[b]	BC019374	4.0
Transport		
ATP-binding cassette, sub-family C (CFTR/MRP), member 12	BB013432	9.2
Hephaestin	NM_010417	9.2
CD36 antigen	AK004192	8.6
ATP-binding cassette, sub-family C (CFTR/MRP), member 5	BB436535	6.5
Solute carrier family 1 (neuronal/epithelial high-affinity glutamate transporter, system Xag), member 1	U75214	4.9
Nucleoporin 93	BC023140	4.9
Immunological proteins		
Attractin	NM_009730	21
Lymphocyte antigen 6 complex, locus D	NM_010742	17
Platelet/endothelial cell adhesion molecule 1	NM_008816	12
Lipocalin 2	X14607	5.3
Chemokine (C–C motif) ligand 9	AF128196	4.6
Signal transduction		
Prostaglandin F receptor	NM_008966	15
Guanylate cyclase 2c	AI893437	14
RAB11 family interacting protein 4 (class II)	BB046187	9.8
Acidic (leucine-rich) nuclear phosphoprotein 32 family, member A	AF022957	9.2
Prominin 1	NM_008935	6.1
Protein phosphatase 1, regulatory (inhibitor) subunit 12A	BI653999	4.9
Cyclin T1	BF538435	4.9
Protein kinase C, ν	NM_029239	4.3
Miscellaneous		
Hydroxyacid oxidase (glycolate oxidase) 3	NM_019545	97
Oxysterol binding protein-like 3	AK004768	74
Tubulointerstitial nephritis antigen	BC010745	37
Serine (or cysteine) proteinase inhibitor, clade B, member 1a	AF426024	34
Annexin A13	BC013521	26
Ubiquitin-specific protease 34	BM235696	20
p300/CBP-associated factor	NM_020005	16
Sialyltransferase 10 (α-2,3-sialyltransferase VI)	NM_018784	9.8
Fms interacting protein	AK006840	8.6
NIMA (never in mitosis gene a)-related expressed kinase 4	BF181187	7.5
Dopachrome tautomerase	NM_010024	4.9
Butyrylcholinesterase	NM_009738	4.6
Ectonucleoside triphosphate diphosphohydrolase 5	AF136571	4.3

[a] Numbers indicate the fold-change in gene expression of *Alb-Cre::keap1*$^{flox/-}$ livers relative to that of control *Alb-Cre::keap1*$^{+/+}$ livers. The genes included in the list show over 4.0-fold induction in *Alb-Cre::keap1*$^{flox/-}$ mice compared to *Alb-Cre::keap1*$^{+/+}$ mice (*Alb-Cre::keap1*$^{flox/-}$/*Alb-Cre::keap1*$^{+/+}$ > 4.0).
[b] Which are well-characterized Nrf2–ARE target genes (see Results).

characterized Nrf2–ARE target genes, such as *nqo1* [9,14,19,32–34], *gstmu3* [32,33,35], *gstmu4* [36], *gstmu6* [35,36], *gpx2* [34], *gstalpha2* [32,36], and *gclc* [14,19,32,33,36]. Upon our search in the upstream region of each gene up to 10 kbp, AREs were found in all the genes listed in Table 1 except for *sult2a2* and *mrp5*.

To verify the microarray data, we examined mRNA abundance of representative genes in livers of *Alb-Cre::keap1*$^{+/+}$ and *Alb-Cre::keap1*$^{flox/-}$ mice. We found by RT-PCR analysis that mRNAs for SULT3A1, Cbr3, Gpx2, GSTmu3, GSTmu4, and GSTmu6 were overexpressed in *Alb-Cre::keap1*$^{flox/-}$ livers as observed in the microarray analysis (Fig. 3C). In addition to the 15 genes identified in the microarray, *ugt1a10*, one of detoxifying enzymes catalyzing glucuronidation, was additionally found to be upregulated in the absence of Keap1 (Fig. 3C). All these genes, including *ugt1a10*, possess AREs in their regulatory regions and must be activated by Nrf2 that escaped from the suppression by Keap1 (Fig. 4B, upper panel).

Diversified regulation of Nrf2–ARE pathway-dependent genes

We have noticed in the microarray analysis that several genes regarded as Nrf2–ARE pathway-dependent genes were not induced or only marginally induced in livers of *Alb-Cre::keap1*$^{flox/-}$ mice. This group of genes includes *ho-1*, *prdx1*, and *gclm* (Fig. 4A). RNA blot analysis of total RNAs from *Alb-Cre::keap1*$^{+/+}$ and *Alb-Cre::keap1*$^{flox/-}$ mouse livers showed apparent induction of *gclc* and *ugt1a6* (Fig. 4A, upper half), which was consistent with the previous report after the stimulation with electrophiles or oxidants [26,32–34]. In contrast, only slight induction of *prdx1* gene expression was observed in *Alb-Cre::keap1*$^{flox/-}$ livers, and the expression levels of HO-1 and GCLM mRNAs were indistinguishable between the two lines of mice (Fig. 4A, lower half).

The unexpectedly mild or no increase of three genes (*ho-1*, *prdx1*, and *gclm*) in *Alb-Cre::keap1*$^{flox/-}$ mouse livers suggests that there may be extensive diversity in the regulatory mechanisms of the ARE-dependent genes in vivo, and multiple dimensions comprise the diversity in the ARE-dependent regulations. For instance, we envisage that the three genes refractory to this genetic induction might use different machineries. First, the lack of the *ho-1* gene induction seems to be attributable to the presence of a repressor protein Bach1 that interacts with AREs in the *ho-1* gene [37]. Simple overdose of Nrf2 may not be sufficient to compete effectively against Bach1 [37], but certain direct effects of electrophiles/oxidants on the Bach1 regulatory pathway may be mandatory for abolishing repressive Bach1 activity. Second, marginal induction of *prdx1* gene seems to be attributable to the difference in cell lineages. The present result suggests that, in contrast to the intensive induction of *prdx1* gene in the primary culture of peritoneal macrophages [27], the capacity of hepatocytes for expressing *prdx1* gene may be limited. Third, the lack of increase in *gclm* expression in *Alb-Cre::keap1*$^{flox/-}$ livers implies that mere accumulation of Nrf2 in the nucleus may not be sufficient to activate certain types of ARE-dependent genes (Fig. 4B, lower panel). Additional modification of Nrf2 and/or recruitment of co-activators provoked by the inducers may be required (see Discussion).

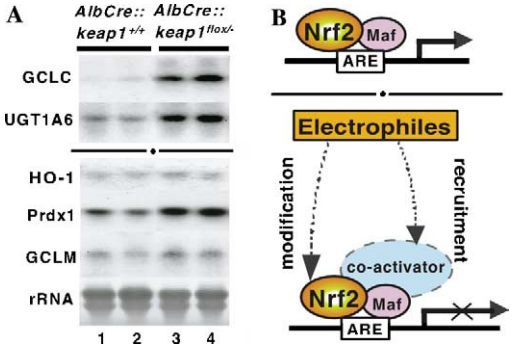

Fig. 4. Diversified effects of hepatocyte-specific *keap1* inactivation on expression level of typical ARE-dependent genes. (A) RNA blot analysis showing ARE-dependent gene expression in *Alb-Cre::keap1*$^{+/+}$ (lanes 1 and 2) and *Alb-Cre::keap1*$^{flox/-}$ mouse livers (lanes 3 and 4). Abundance of ribosomal RNA was monitored as loading controls. (B) Schematic illustration of two ways of ARE-dependent gene regulation. (top) Genes readily activated by Nrf2 that escaped from repression by Keap1. (bottom) Genes requiring additional signals, including Nrf2 modification and co-activator recruitment, for being activated by Nrf2.

Hepatocyte-specific deletion of keap1 gene and acetaminophen-induced hepatotoxicity

The contribution of Nrf2 to the protection against xenobiotic toxicity has been shown in studies of *nrf2*$^{-/-}$ animals which are highly susceptible to the acute toxicity caused by APAP and other chemicals [11,12]. However, although these analyses gave rise to consistent results, some pertinent issues remain to be addressed. First, there is no conclusive evidence that hepatocyte-specific enhancement of Nrf2 activity is actually effective in promoting xenobiotic resistance. Second, there is a possibility that pharmacological inducers exert their effects by activating other regulatory pathways apart from the Nrf2–ARE pathway. To clarify these points, we examined the susceptibility of *Alb-Cre::keap1*$^{flox/-}$ mice to APAP-induced hepatotoxicity.

Following intraperitoneal administration of 600-mg or 700-mg APAP/kg body weight, most of the *Alb-Cre::keap1*$^{+/+}$ mice died. In stark contrast, all *Alb-Cre::keap1*$^{flox/-}$ mice survived the challenge (Fig. 5A). Serum ALT levels correlated well with the survival rates, remaining low in the *Alb-Cre::keap1*$^{flox/-}$ mice (Table 2). An assessment of the surviving animals 48 h after APAP treatment by histological examination showed much milder hepatic injury in livers of *Alb-Cre::keap1*$^{flox/-}$ mice compared to *Alb-Cre::keap1*$^{+/+}$ mice (compare Figs. 5B and C). In *Alb-Cre::keap1*$^{+/+}$ livers, central veins were surrounded by bands of massive necrotic hepatocytes, while morphological integrity of hepatocytes was mostly preserved in *Alb-Cre::keap1*$^{flox/-}$ livers.

To examine whether the susceptibility to APAP toxicity was associated with the extent of the covalent binding of acetaminophen metabolites to liver proteins, we performed immunohistochemical staining using an antibody

A Survival Rate of Mice 48hr after Administration of APAP

genotype	APAP 700mg/kg	APAP 600mg/kg	Saline control
AlbCre::keap1$^{+/+}$	0/4	1/4	4/4
AlbCre::keap1$^{flox/-}$	3/3	3/3	4/4

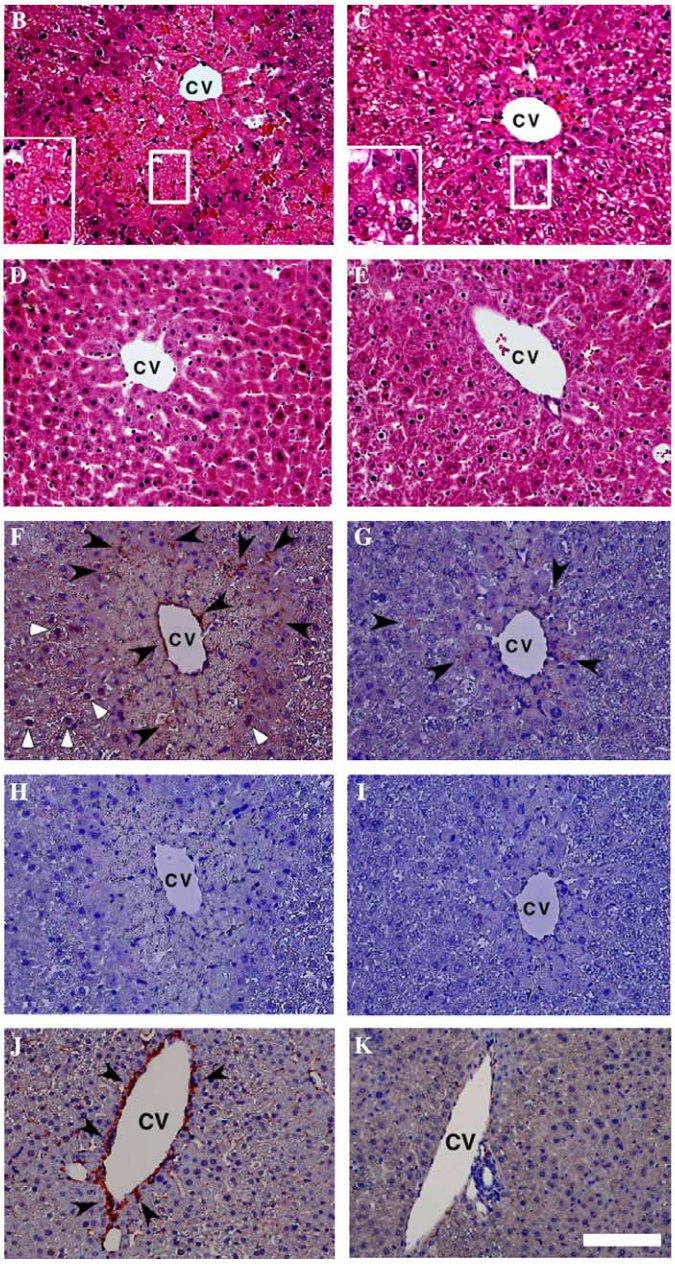

Fig. 5. *Alb-Cre::keap1*$^{flox/-}$ mice are more resistant to acute hepatotoxicity of APAP. (A) Survival rate of mice after APAP administration. Numerators and denominators indicate the numbers of survived mice and of tested mice, respectively. (B–I) Liver sections of mice sacrificed 48 h after the administration of 600-mg/kg APAP (B,C,F,G) or vehicle (saline) (D,E,H,I). The sections were stained with hematoxylin and eosin (B–E) or reacted with anti-APAP–protein adduct antibody to detect APAP–adduct formation (F–I). Centrilobular hepatic necrosis is much milder in *Alb-Cre::keap1*$^{flox/-}$ liver (C) than in wild-type liver (B). Higher magnifications of rectilinear regions with white lines are shown as insets (B,C). Immunoreactivity with anti-APAP antibody is very intense in the section of *Alb-Cre::keap1*$^{+/+}$ liver (F), while only weaker signals are observed in *Alb-Cre::keap1*$^{flox/-}$ liver (G). Positive signals detected in cytoplasm and nucleus are marked with closed and open arrowheads, respectively. *Alb-Cre::keap1*$^{+/+}$ and *Alb-Cre::keap1*$^{flox/+}$ livers treated with saline are shown in (D,H) and (E,I), respectively. (J,K) Response to a sub-lethal dose of APAP. Accumulation of APAP adducts was detected with anti-APAP antibody in *Alb-Cre::keap1*$^{+/+}$ (J) and *Alb-Cre::keap1*$^{flox/-}$ (K) livers 5 h after administration of 500-mg/kg APAP. Centrilobular necrosis is not observed in both sections. Strong signals are detected in the endothelial cells surrounding the central vein (indicated with closed arrowheads) and hepatocyte nuclei are also weakly stained in *Alb-Cre::keap1*$^{+/+}$ mouse liver (J). No such signal is observed in *Alb-Cre::keap1*$^{flox/-}$ liver (K). Scale bar corresponds to 100 μm (B–K). cv, central vein.

Table 2
Plasma ALT activity 48 h after the administration of APAP

Genotype	APAP 700 mg/kg	APAP 600 mg/kg	Saline control
Alb-Cre::keap1$^{+/+}$	ND	>1000	102 ± 44.9[a]
	ND	ND	
	ND	ND	
	ND	ND	
Alb-Cre::keap1$^{flox/-}$	>1000	285 ± 39[c]	58 ± 77.9[b]
	>1000		
	891		

Average values and the standard deviations were calculated when the ALT activity was measured in more than three animals of the same genotype with the same dose.
ND: Plasma ATP levels could not be measured because mice died within 48 h of APAP administration.
[a] Five independent mice were examined.
[b] Four independent mice were examined.
[c] Three independent mice were examined.

against APAP–protein adducts. The signal intensity was much stronger in *Alb-Cre::keap1*$^{+/+}$ mice than in *Alb-Cre::keap1*$^{flox/-}$ mice (compare Figs. 5F and G). In *Alb-Cre::keap1*$^{+/+}$ liver, intense brownish signals were evident in endothelial cells of central veins and in hepatocytes surrounding the necrotic areas. These results thus indicate that the formation of APAP–protein adducts was largely repressed in *Alb-Cre::keap1*$^{flox/-}$ livers compared with that of *Alb-Cre::keap1*$^{+/+}$ livers.

To clarify how Keap1-deficient hepatocytes respond effectively to the APAP hepatotoxicity, we next treated both *Alb-Cre::keap1*$^{flox/-}$ and *Alb-Cre::keap1*$^{+/+}$ mice with sub-lethal dose of APAP (500 mg/kg) and examined the early phase response. While the APAP-adduct formation was not evident in the livers of both *Alb-Cre::keap1*$^{flox/-}$ and *Alb-Cre::keap1*$^{+/+}$ mice by 2 h (data not shown), we could detect clear signals of the APAP-adduct formation in *Alb-Cre::keap1*$^{+/+}$ livers at 5 h after the treatment (Fig. 5J). Importantly, however, no such signal was detected in *Alb-Cre::keap1*$^{flox/-}$ mouse livers (Fig. 5K). These results suggest that APAP-metabolizing pathways are activated and reactive intermediates are effectively removed in the livers of *Alb-Cre::keap1*$^{flox/-}$ mice.

Discussion

In this study, we observed that somatic disruption of *keap1* does not interfere with the development or the morphological and physiological integrity of the liver. Our microarray analysis showed that genetic disruption of the *keap1* gene induced overlapping but clearly distinct sets of drug-metabolizing enzymes from those induced by exogenous chemicals. Through the induction of detoxifying enzymes, specific knockout of the *keap1* gene confers hepatocytes with a strong resistance to drug-induced toxicity. Considering the tight relationship between Keap1 and Nrf2, these results support our contention that the constitutive activation of Nrf2, and concomitantly its target genes, is advantageous for animals to overcome xenobiotic toxicity.

To identify genes regulated by the Nrf2–ARE pathway, hepatic gene expression profiles were previously examined by microarray analysis of vehicle or 3*H*-1,2-dithiole-3-7thione (D3T)-treated wild-type mice as well as in *nrf2* knockout mice [32]. D3T is a potent Nrf2 inducer and resulted in elevated transcript levels for 292 genes in wild-type mice 24 h after treatment with D3T. Of these genes, 79% were induced in wild-type mice, but not in *nrf2*-deficient mice [32]. These *nrf2*-dependent, D3T-inducible genes included known detoxication and antioxidative enzymes, indicating that D3T increases the expression of genes through the Nrf2–ARE signaling pathway that directly eliminate reactive toxins or generate essential cofactors such as glutathione and reducing equivalents for their detoxification. Unexpected clusters included genes for chaperones, protein trafficking, ubiquitin/26S proteasome subunits, and signaling molecules, suggesting that the induction of *nrf2*-dependent genes is involved in the recognition and repair/removal of damaged proteins. Consistent with these observations, the present microarray analysis also revealed that the expression levels of the detoxication genes are, in general, highly elevated in *Alb-Cre::keap1*$^{flox/-}$ mouse hepatocytes.

Upon closer comparison of the genes induced by the exogenous chemical agent and those induced by genetic ablation of Keap1 expression, a number of interesting features were unveiled. One is that, in the present microarray analysis, the elevation of *prdx1* gene expression was only marginal and no significant changes were observed in the levels of *gclm* and *ho-1* gene expression. They are well-characterized ARE-dependent genes [19,27,32,33] and shown to be induced by D3T in mouse liver [32]. The other is that expression levels of the genes related to the proteasome function, which were found to be induced by D3T [32], did not show significant change in the *Alb-Cre::keap1*$^{flox/-}$ livers.

We surmise that the following observations may be pertinent in explaining these observations. In the previous microarray analysis, we used mice in which Nrf2 expression was likely induced in multiple cell types within the liver in addition to hepatocytes by D3T, while in the present analysis we used mice in which the *keap1* gene was disrupted solely in hepatocytes. Therefore, there may be genes that are preferentially induced in hepatocytes or preferentially induced in the other types of liver cells that account for the differences observed between the present and previous microarray analyses (e.g., *prdx1* in Fig. 4A). Alternatively, the possibility exists that treatment of animals with the exogenous chemical D3T might induce other signaling pathways that further potentiate the Nrf2 activity (modification of Nrf2 and/or co-activator recruitment; see Fig. 4B) or that are not related to Nrf2. Since the present analysis represents a genetic activation of Nrf2, differences in the gene expression profiles between the present and previous analysis might be due to additional signals for achieving full activation of Nrf2 or due to specific signals

transduced by pathways other than that mediated by Nrf2. Thus, our present study provides a unique and simplified model system of Nrf2 activation, and we believe that the comparative analysis of the xenobiotic induction and genetic induction of the Nrf2-dependent genes will give us a new insight into the inducible mechanisms of the cytoprotective genes.

The expression profile of the *ho-1* gene in *Alb-Cre::keap1*$^{flox/-}$ mouse liver is intriguing. Whereas expression of the *ho-1* gene is highly inducible by electrophiles, oxidants, and heavy metals, somewhat surprisingly the gene is not induced in hepatocytes of the *Alb-Cre::keap1*$^{flox/-}$ mouse. Thus, a difference exists between chemical and genetic induction of the *ho-1* gene. As both genetic and biochemical lines of evidence suggest the presence of a negative contribution by Bach1 to *ho-1* gene regulation [37], we speculate that, in addition to the increase of Nrf2, liberation from Bach1-mediated repression may also be required for *ho-1* gene expression in *Alb-Cre::keap1*$^{flox/-}$ hepatocytes.

To evaluate the functional consequence of a continuous induction of a battery of ARE-dependent genes in liver, we assessed the susceptibility to APAP-induced hepatotoxicity. The critical detoxification process is the elimination of the reactive metabolite NAPQI, which is mediated by GSTs, typical ARE-dependent gene products [23]. As predicted, we found that the *Alb-Cre::keap1*$^{flox/-}$ mice were highly resistant to the toxicity of APAP. Other APAP-metabolizing pathways, most likely sulfation and glucuronidation, seem to contribute to the enhanced resistance. Indeed, we found that total mRNAs for UGT1 family genes were markedly increased in the absence of Keap1 (data not shown). Among the UGT1 family subtypes, UGT1A6 and UGT1A10 were highly expressed. *Ugt1a6* is reported as one of the ARE-dependent genes regulated by Nrf2 [26] and *ugt1a10* possesses several ARE sequences in its promoter region, suggesting that the glucuronidation pathway is regulated by Nrf2 and its activity is elevated in the *Alb-Cre::keap1*$^{flox/-}$ hepatocytes.

In contrast, the expression of *sult1a1* gene, an enzyme responsible for sulfation of phenolic compounds [38], did not change significantly (fold induction = 1.2) in the microarray analysis. Although *sult2a2* and *sult3a1* genes were dramatically induced in *Alb-Cre::keap1*$^{flox/-}$ mice (Table 1), these isozymes are suboptimal enzymes for the metabolism of APAP. We conclude from these analyses that both the glutathione and UDP–glucuronide pathways may contribute to the enhanced capacity of *Alb-Cre::keap1*$^{flox/-}$ hepatocytes to eliminate APAP, although detailed examination of the metabolites and intermediates of APAP will be necessary for full characterization of the effects of the *Alb-Cre::keap1*$^{flox/-}$ genotype on APAP disposition.

A recent toxicogenomic report utilized the Nrf2-dependent pathway as a parameter for categorizing various hepatotoxins as regulators of PPARα and NFκB pathways [39]. The report nicely complements our contention that the Nrf2–ARE pathway comprises one of the major transcriptional response mechanisms directed towards an adaptive response against xenobiotic stress. In turn, our present data provide a rationale for the molecular basis of this type of analysis. Being aware that Nrf2-mediated gene activation might not be sufficiently effective to impose resistance against PPARα and/or NFκB chemical activators, we consider Nrf2 as a good intervention target to promote detoxification ability in the liver.

Acknowledgments

We thank Drs. K. Araki and K. Yamamura for providing us AYU1-Cre transgenic mice and Dr. S. Yamamoto for giving us advice on microarray data interpretation. We also thank Ms. N. Kaneko and R. Kawai for experimental assistance and Dr. V. Kelley for English edition. This work was supported by grants from the Ministry of Education, Science, Sports and Culture (H.M. and M.Y.), the Uehara Memorial Foundation (H.M.), Yamanouchi Foundation (H.M.), Atherosclerosis Foundation (M.Y.), and ERATO-JST (M.Y.).

References

[1] U.A. Meyer, Overview of enzymes of drug metabolism, J. Pharmacokinet. Biopharm. 5 (1996) 449–459.
[2] T.W. Kensler, G.S. Qian, J.G. Chen, J.D. Groopman, Translational strategies for cancer prevention in liver, Nat. Rev. Cancer 5 (2003) 321–329.
[3] J.D. Hayes, M. McMahon, Molecular basis for the contribution of the antioxidant responsive element to cancer chemoprevention, Cancer Lett. 174 (2001) 103–113.
[4] P. Talalay, Mechanisms of induction of enzymes that protect against chemical carcinogenesis, Adv. Enzyme Regul. 28 (1989) 237–250.
[5] E.M. Leslie, R.G. Deeley, S.P. Cole, Multidrug resistance proteins: role of P-glycoprotein, MRP1, MRP2, and BCRP (ABCG2) in tissue defense, Toxicol. Appl. Pharmacol. 204 (2005) 216–237.
[6] H. Motohashi, T. O'Connor, F. Katsuoka, J.D. Engel, M. Yamamoto, Integration and diversity of the regulatory network composed of Maf and CNC families of transcription factors, Gene 294 (2002) 1–12.
[7] K. Itoh, K. Igarashi, N. Hayashi, M. Nishizawa, M. Yamamoto, Cloning and characterization of a novel erythroid cell-derived CNC family transcription factor heterodimerizing with the small Maf family proteins, Mol. Cell. Biol. 8 (1995) 4184–4193.
[8] H. Motohashi, F. Katsuoka, J.D. Engel, M. Yamamoto, Small Maf proteins serve as transcriptional cofactors for keratinocyte differentiation in the Keap1–Nrf2 regulatory pathway, Proc. Natl. Acad. Sci. USA 101 (2004) 6379–6384.
[9] K. Itoh, T. Chiba, S. Takahashi, T. Ishii, K. Igarashi, Y. Katoh, T. Oyake, N. Hayashi, K. Satoh, I. Hatayama, M. Yamamoto, Y. Nabeshima, An Nrf2/small Maf heterodimer mediates the induction of phase II detoxifying enzyme genes through antioxidant response elements, Biochem. Biophys. Res. Commun. 236 (1997) 313–322.
[10] A. Hayashi, H. Suzuki, K. Itoh, M. Yamamoto, Y. Sugiyama, Transcription factor Nrf2 is required for the constitutive and inducible expression of multidrug resistance-associated protein 1 in mouse embryo fibroblasts, Biochem. Biophys. Res. Commun. 310 (2003) 824–829.
[11] A. Enomoto, K. Itoh, E. Nagayoshi, J. Haruta, T. Kimura, T. O'Connor, T. Harada, M. Yamamoto, High sensitivity of Nrf2 knockout mice to acetaminophen hepatotoxicity associated with decreased expression of ARE-regulated drug metabolizing enzymes and antioxidant genes, Toxicol. Sci. 59 (2001) 169–177.

[12] K. Chan, X.D. Han, Y.W. Kan, An important function of Nrf2 in combating oxidative stress: detoxification of acetaminophen, Proc. Natl. Acad. Sci. USA 98 (2001) 4611–4616.
[13] Y. Aoki, H. Sato, N. Nishimura, S. Takahashi, K. Itoh, M. Yamamoto, Accelerated DNA adduct formation in the lung of the Nrf2 knockout mouse exposed to diesel exhaust, Toxicol. Appl. Pharmacol. 173 (2001) 154–160.
[14] K. Chan, Y.W. Kan, Nrf2 is essential for protection against acute pulmonary injury in mice, Proc. Natl. Acad. Sci. USA 96 (1999) 12731–12736.
[15] K. Itoh, N. Wakabayashi, Y. Katoh, T. Ishii, K. Igarashi, J.D. Engel, M. Yamamoto, Keap1 represses nuclear activation of antioxidant responsive elements by Nrf2 through binding to the amino-terminal Neh2 domain, Genes Dev. 13 (1999) 76–86.
[16] A. Kobayashi, T. Ohta, M. Yamamoto, Unique function of the Nrf2–Keap1 pathway in the inducible expression of antioxidant and detoxifying enzymes, Methods Enzymol. 378 (2004) 273–286.
[17] H. Motohashi, M. Yamamoto, Nrf2–Keap1 defines a physiologically important stress response mechanism, Trends Mol. Med. 11 (2004) 549–557.
[18] A. Kobayashi, M.-I. Kang, H. Okawa, M. Ohtsuji, Y. Zenke, T. Chiba, K. Igarashi, M. Yamamoto, Oxidative stress sensor Keap1 functions as an adaptor for Cul3-based E3 ligase to regulate proteasomal degradation of Nrf2, Mol. Cell. Biol. 16 (2004) 7130–7139.
[19] N. Wakabayashi, K. Itoh, J. Wakabayashi, H. Motohashi, S. Noda, S. Takahashi, S. Imakado, T. Kotsuji, F. Otsuka, D.R. Roop, T. Harada, J.D. Engel, M. Yamamoto, Keap1-null mutation leads to postnatal lethality due to constitutive Nrf2 activation, Nat. Genet. 35 (2003) 238–245.
[20] L.F. Prescott, Paracetamol overdosage. Pharmacological considerations and clinical management, Drugs 25 (1983) 290–314.
[21] M. Patel, B.K. Tang, W. Kalow, Variability of acetaminophen metabolism in Caucasians and Orientals, Pharmacogenetics 2 (1992) 38–45.
[22] N.P. Vermeulen, J.G. Bessems, R. Van de Straat, Molecular aspects of paracetamol-induced hepatotoxicity and its mechanism-based prevention, Drug Metab. Rev. 24 (1992) 367–407.
[23] L.P. James, P.R. Mayeux, J.A. Hinson, Acetaminophen-induced hepatotoxicity, Drug Metab. Dispos. 12 (2003) 1499–1506.
[24] S.S. Ansher, P. Dolan, E. Bueding, Chemoprotective effects of two dithiolthiones and of butylhydroxyanisole against carbon tetrachloride and acetaminophen toxicity, Hepatology 3 (1983) 932–935.
[25] K.W. Seo, J.G. Kim, M. Park, T.W. Kim, H.J. Kim, Effects of phenethylisothiocyanate on the expression of glutathione *S*-transferases and hepatotoxicity induced by acetaminophen, Xenobiotica 30 (2000) 535–545.
[26] K. Iida, K. Itoh, Y. Kumagai, R. Oyasu, K. Hattori, K. Kawai, T. Shimazui, H. Akaza, M. Yamamoto, Nrf2 is essential for the chemopreventive efficacy of oltipraz against urinary bladder carcinogenesis, Cancer Res. 64 (2004) 6424–6431.
[27] T. Ishii, K. Itoh, E. Ruiz, D.S. Leake, H. Unoki, M. Yamamoto, G.E. Mann, Role of Nrf2 in the regulation of CD36 and stress protein expression in murine macrophages: activation by oxidatively modified LDL and 4-hydroxynonenal, Circ. Res. 94 (2004) 609–616.
[28] J.D. Dignam, Preparation of extracts from higher eukaryotes, Methods Enzymol. 182 (1990) 194–203.
[29] M.-I. Kang, A. Kobayashi, N. Wakabayashi, M. Yamamoto, Scaffolding of Keap1 to the actin cytoskeleton controls the function of Nrf2 as key regulator of cytoprotective phase 2 genes, Proc. Natl. Acad. Sci. USA 101 (2004) 2046–2051.
[30] N. Wakabayashi, A.T. Dinkova-Kostova, W.D. Holtzclaw, M.-I. Kang, A. Kobayashi, M. Yamamoto, T.W. Kensler, P. Talalay, Protection against electrophile and oxidant stress by induction of the phase 2 response: fate of cysteines of the Keap1 sensor modified by inducers, Proc. Natl. Acad. Sci. USA 101 (2004) 2040–2045.
[31] H. Niwa, K. Araki, S. Kimura, S. Tanigushi, S. Wakasugi, K. Yamamura, An efficient gene-trap method using poly A trap vectors and characterization of gene-trap events, J. Biochem. 113 (1993) 343–349.
[32] M.-K. Kwak, N. Wakabayashi, K. Itoh, H. Motohashi, M. Yamamoto, T.W. Kensler, Modulation of gene expression by cancer chemopreventive dithiolethiones through the Keap1–Nrf2 pathway. Identification of novel gene clusters for cell survival, J. Biol. Chem. 278 (2003) 8135–8145.
[33] J.M. Lee, M.J. Calkins, K. Chan, Y.W. Kan, J.A. Johnson, Identification of the NF-E2-related factor-2-dependent genes conferring protection against oxidative stress in primary cortical astrocytes using oligonucleotide microarray analysis, J. Biol. Chem. 278 (2003) 12029–12038.
[34] H.Y. Cho, A.E. Jedlicka, S.P. Reddy, T.W. Kensler, M. Yamamoto, L.Y. Zhang, S.R. Kleeberger, Role of NRF2 in protection against hyperoxic lung injury in mice, Am. J. Respir. Cell Mol. Biol. 26 (2002) 175–182.
[35] Z. Xu, L. Chen, L. Leung, T.S. Yen, C. Lee, J.Y. Chan, Liver-specific inactivation of the Nrf1 gene in adult mouse leads to nonalcoholic steatohepatitis and hepatic neoplasia, Proc. Natl. Acad. Sci. USA 102 (2005) 4120–4125.
[36] S.A. Chanas, Q. Jiang, M. McMahon, G.K. McWalter, L.I. McLellan, C.R. Elcombe, C.J. Henderson, C.R. Wolf, G.J. Moffat, K. Itoh, M. Yamamoto, J.D. Hayes, Loss of the Nrf2 transcription factor causes a marked reduction in constitutive and inducible expression of the glutathione *S*-transferase Gsta1, Gsta2, Gstm1, Gstm2, Gstm3 and Gstm4 genes in the livers of male and female mice, Biochem. J. 365 (2002) 405–416.
[37] J. Sun, M. Brand, Y. Zenke, S. Tashiro, M. Groudine, K. Igarashi, Heme regulates the dynamic exchange of Bach1 and NF-E2-related factors in the Maf transcription factor network, Proc. Natl. Acad. Sci. USA 101 (2004) 1461–1466.
[38] C.N. Falany, Enzymology of human cytosolic sulfotransferases, FASEB J. 11 (1997) 206–216.
[39] M. McMillian, A. Nie, J.B. Parker, A. Leone, M. Kemmerer, S. Bryant, J. Herlich, L. Yieh, A. Bittner, X. Liu, J. Wan, M.D. Johnson, P. Lord, Drug-induced oxidative stress in rat liver from a toxicogenomics perspective, Toxicol. Appl. Pharmacol. 207 (2005) S171–S178.